

# Mechanical disruption of individual nucleosomes reveals a reversible multistage release of DNA

Brent D. Brower-Toland\*, Corey L. Smith<sup>†</sup>, Richard C. Yeh\*, John T. Lis<sup>‡</sup>, Craig L. Peterson<sup>†</sup>, and Michelle D. Wang\*<sup>§</sup>

\*Department of Physics, Laboratory of Atomic and Solid State Physics, and <sup>‡</sup>Department of Molecular Biology and Genetics, Cornell University, Ithaca, NY 14853; and <sup>†</sup>Program in Molecular Medicine, University of Massachusetts Medical School, Worcester, MA 01605

Communicated by Jeffrey W. Roberts, Cornell University, Ithaca, NY, November 30, 2001 (received for review September 24, 2001)

**The dynamic structure of individual nucleosomes was examined by stretching nucleosomal arrays with a feedback-enhanced optical trap. Forced disassembly of each nucleosome occurred in three stages. Analysis of the data using a simple worm-like chain model yields 76 bp of DNA released from the histone core at low stretching force. Subsequently, 80 bp are released at higher forces in two stages: full extension of DNA with histones bound, followed by detachment of histones. When arrays were relaxed before the dissociated state was reached, nucleosomes were able to reassemble and to repeat the disassembly process. The kinetic parameters for nucleosome disassembly also have been determined.**

Nucleosomes are the fundamental organizational unit of the eukaryotic genome, occurring on average every 200 bp (1). The foundation of the nucleosome is the nucleosome core particle (NCP), consisting of 147 bp of DNA wrapped 1.65 times around an octamer of histone proteins (2). The NCP must be a stable and yet dynamic structure, both maintaining eukaryotic DNA in a condensed state and also permitting regulated access to genetic information contained therein. Equilibrium accessibility of DNA in the NCP has been demonstrated by using restriction enzyme accessibility assays (3). As visualized by cryoelectron microscopy, variability in the amount of DNA associated with the histone octamer and in the angle of exit and entry of DNA from the NCP are also consistent with spontaneous peeling of DNA ends from the octamer surface (4). Spontaneous peeling presents a means by which the transcriptional apparatus might invade nucleosomal DNA, especially if this process were facilitated by force-generating molecular motors and destabilizing covalent histone modifications.

Single-molecule mechanical manipulation techniques offer a direct approach to the investigation of the forces and displacements required for enzymatic access to nucleosome-bound DNA. These techniques already have provided insights into the higher-order structure of chromatin fibers and the kinetics of fiber assembly (5, 6); however, the resolution of these studies has not permitted observations of the interactions within individual nucleosomes. Bennink *et al.* (7) used optical tweezers to stretch single chromatin fibers assembled with *Xenopus* oocyte extracts on  $\lambda$  phage DNA. Although their force-extension curves do not show a periodic pattern of DNA release (as might be expected of individual nucleosomal disruption events), analysis of the data allowed them to arrive at an  $\approx 65$  nm ( $\approx 190$  bp) “quantization” in chromatin opening which they attribute to the sudden unwrapping of DNA from individual histone octamers. The abundance of linker histone-like proteins B4, HMG1, HMG2 (8), and other non-histone chromatin-associated proteins in oocyte nuclear extracts used for chromatin assembly in these experiments may in part explain the lack of uniformity and periodicity in the force-extension profiles displayed for chromatin disruption. This lack of uniformity would, in turn, complicate the identification of individual nucleosome disruption signatures.

In the current study, we have used a well defined system to study the dynamic structure of individual nucleosomes: chromatin arrays reconstituted with purified core histones on a DNA containing repeating units of the 5S rRNA nucleosome posi-

tioning element. We report here observations of individual nucleosome disruption events on these arrays obtained with a feedback-enhanced optical trap. Single nucleosomal arrays were stretched in one of two feedback modes to disrupt DNA-histone interactions dynamically. Our results suggest a model in which DNA in the nucleosome is released in three stages, which reflect DNA-protein interactions with different chemical stabilities. This model is consistent with and extends published biochemical and structural data on DNA-histone interactions in nucleosomes (1–4) and provides insight into the nature of enzymatic mechanisms that require access to nucleosomal DNA.

## Materials and Methods

**Nucleosomal Array Preparation.** Nucleosomal arrays were prepared with avian core histones and a 3,684 bp DNA fragment containing 17 direct tandem repeats of the sea urchin 5S positioning element. This naturally occurring sequence has been shown to position a nucleosome at a well defined location (9). Nucleosomal arrays were prepared by using an established method of stepwise dialysis through decreasing salt concentrations (10). Array quality and approximate number of nucleosomes per reconstituted array also were determined with established methods by sedimentation velocity analyses in a Beckman Optima XL-I analytical ultracentrifuge (Beckman Coulter; ref. 11). Protein-protein cross-linking within nucleosomes on minimally saturated arrays was achieved by using dimethyl suberimidate (12).

**Experimental Configuration.** Stretching experiments were carried out in buffer containing 10 mM Tris-HCl (pH 8.0), 1 mM Na<sub>2</sub>EDTA, 100 mM NaCl, 1.5 mM MgCl<sub>2</sub>, 0.02% (vol/vol) Tween 20, and 0.01% (wt/vol) milk protein at 22°C. The DNA fragment was labeled at one end with biotin and at the other end with digoxigenin (Roche Molecular Biochemicals). Before stretching, one end of each nucleosomal array was attached to the surface of an anti-digoxigenin-coated (Roche Molecular Biochemicals) microscope coverslip. A 0.48- $\mu$ m diameter streptavidin-coated polystyrene microsphere (Bangs Laboratories) then was attached to the free end of each tethered array. Individual arrays have rotational freedom at both the bead and surface linkage in this experimental configuration.

Once a surface-tethered microsphere was optically trapped, the coverslip was moved with a piezoelectric stage to stretch the nucleosomal DNA with either a velocity clamp or a force clamp (Fig. 1A). The design and calibration of the setup and the data acquisition methods are similar to those used previously for studies of RNA polymerase as a molecular motor and for kinesin (13–15). In the velocity clamp mode, the coverslip was moved at a constant velocity relative to the microsphere, whose position

Abbreviations: NCP, nucleosome core particle; DFS, dynamic force spectroscopy.

See commentary on page 1752.

<sup>§</sup>To whom reprint requests should be addressed. E-mail: mdw17@cornell.edu.

The publication costs of this article were defrayed in part by page charge payment. This article must therefore be hereby marked “advertisement” in accordance with 18 U.S.C. §1734 solely to indicate this fact.

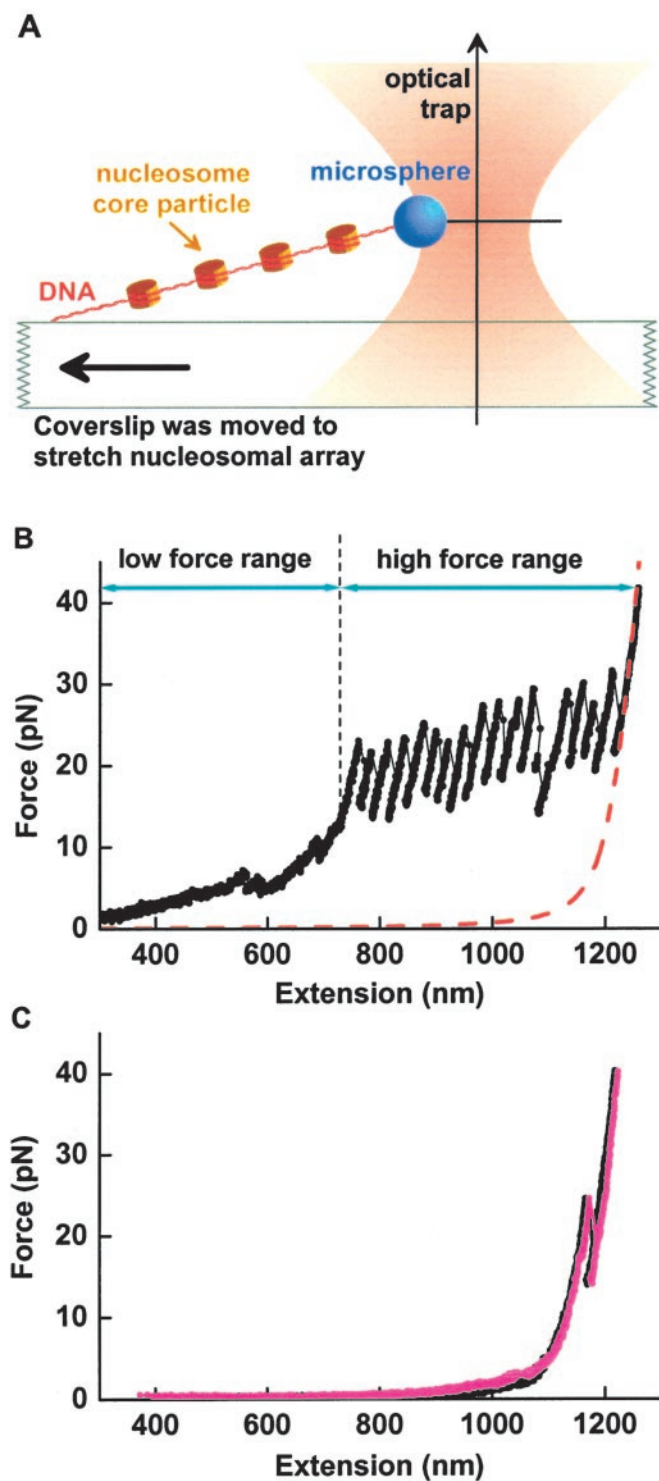


**Fig. 1.** Disruption of individual nucleosomes. (A) Experimental configuration (not to scale). Under feedback control, a nucleosomal array was stretched between the surface of a microscope coverslip and an optically trapped microsphere. Fig. 1 B and C were obtained with a velocity clamp at 28 nm/s. (B) Force-extension curve of a fully saturated nucleosomal array. At higher force (>15 pN), a sawtooth pattern containing 17 disruption peaks was observed. Force-extension characteristics of a full-length naked DNA (red dotted line) is shown for comparison. (C) Force extension curve of nucleosomal arrays containing minimal number of nucleosomes. Overlaid curves are shown for both native (black) and cross-linked (magenta) histone octamers.

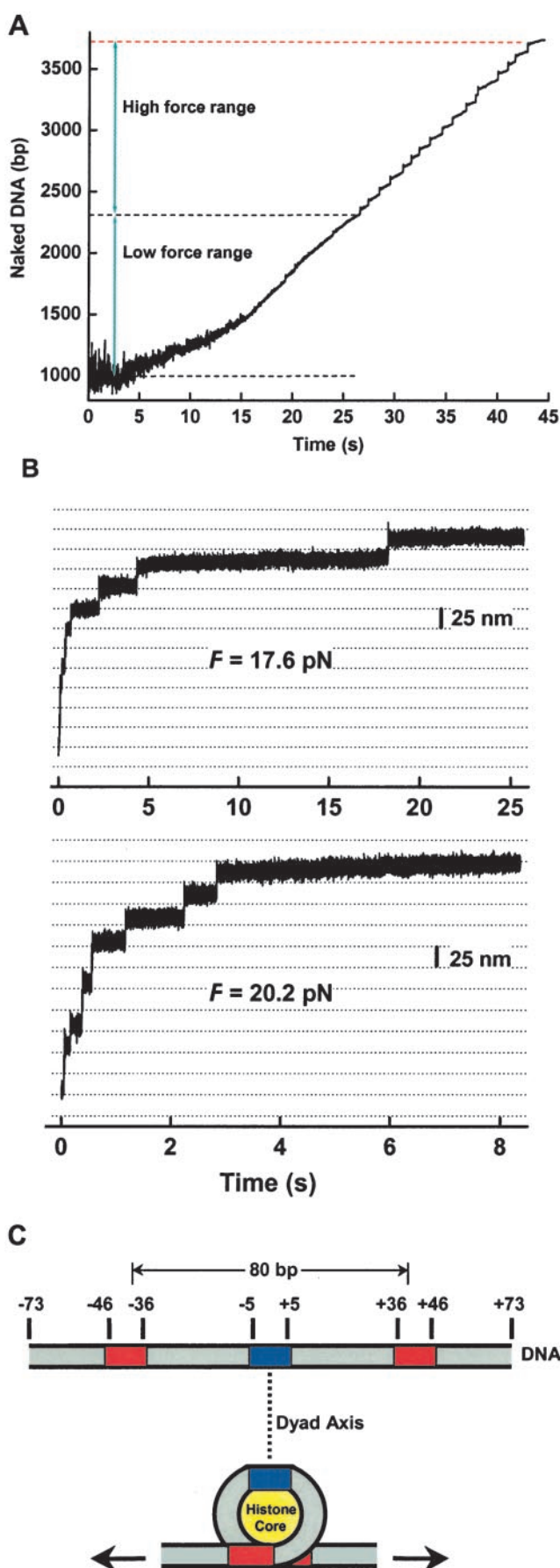
was kept constant by modulating the light intensity (trap stiffness) of the trapping laser. A disruption event, during which DNA was released from an NCP, was observed as a sudden reduction in the tension of the DNA. In the force clamp mode, the position of the coverslip was modulated so that the trapping force was held constant on the microsphere, whose position was fixed in a trap of constant stiffness. In this mode, a disruption event was observed as a step in the coverslip position.

## Results and Discussion

**Observation of Individual Nucleosomal Disruption Events.** Our first set of experiments investigated the disruption of individual nucleosomes by mechanically stretching the nucleosomal DNA as diagramed in Fig. 1A. Examples of force vs. extension curves obtained with a velocity clamp are shown as solid lines with dots for saturated arrays ( $\approx 1$  nucleosome per 5S positioning element; Fig. 1B) and arrays containing a minimal number of nucleosomes (Fig. 1C). In the high-force range (>15 pN), these data show a sawtooth pattern composed of 17 peaks or 1 peak, respectively, for saturated (Fig. 1B) or minimal arrays (Fig. 1C). The sawtooth pattern is reminiscent of that seen upon unraveling tandem repeats of Ig domains in a single titin molecule (16, 17). At the end of the stretch, the chromatin curve approaches that of the full-length naked DNA (dotted line), indicating that no histones remained attached to the DNA in such a way that they would alter DNA elasticity. The 17 peaks indicate disruption of the 17 positioned nucleosomes. At each sawtooth, DNA remained bound until a peak force was reached, leading to a sudden release of DNA and relaxation to a lower tension. Uniform spacing between adjacent peaks ( $\approx 27$  nm) indicates that upon disruption, a relatively constant amount of DNA was released from each NCP. The observed sawtooth pattern suggests sequential disruption of strong DNA-histone interactions in individual nucleosomes. In Fig. 1C, the observation of a single peak is consistent with disruption of a single positioned nucleosome. Furthermore, when histone proteins in these arrays were cross-linked with dimethyl suberimidate, disruption peak characteristics were not changed, indicating that the sawtooth pattern results entirely from DNA-protein bond rupture.

**Determination of the Amount of DNA Release During Disruption.** To quantify the amount of DNA release from a nucleosome, we applied a simple model to our data, attributing extension only to naked DNA (linker DNA and DNA peeled from NCPs). The method of conversion from force-extension curve to number of bp of naked DNA is similar to that used previously for single-molecule studies of transcription (13). Under the buffer conditions used here, the persistence length of DNA was measured at 42 nm and the stretch modulus was 1300 pN, which is in good agreement with previous results under similar buffer conditions (18). Analysis of the saturated-array data in Fig. 1B is shown in Fig. 2A, where the amount of naked DNA is plotted as a function of time during stretching. Between 0–2 s, the average amount of naked DNA is constant, indicating no DNA release from NCPs. Subsequently, DNA is released from the 17 NCPs, producing an increase in the amount of naked DNA from  $\approx 1,000$  bp at the beginning of the stretch to approximately the expected full length of 3,684 bp at the end of the stretch. This finding corresponds to a release of 158 bp of DNA per NCP. This value is within 7% of the canonical value of 147 bp DNA in the core particle determined from the crystal structure (19); the apparent discrepancy may, in fact, reflect a difference between the crystal structure and dynamic nature of solution structures (20). Nucleosomal-DNA release is bipartite, with 76 bp released in the low-force range, and 82 bp released at high force.

In the low-force range, DNA release is gradual. Furthermore, a lack of recognizable disruption peaks (Fig. 1B) and steps (Fig. 2A) in this range indicates a smooth energy landscape as well as



simultaneous release of DNA from all NCPs. The low force required for DNA release in this range indicates that relatively weak DNA–histone interactions were disrupted, whereas the positive slope of the force–extension curve reflects the disruption of progressively stronger DNA–histone interactions. The low-force results are in keeping with the heterogeneity in reported values for nucleosomal-DNA length, which one may attribute to the dynamic nature of the nucleosomal-DNA ends (20). The partial release of DNA from the NCPs in this low-force range was reversible (data not shown) and thus is a quasi-equilibrium process. The free energy of dissociation of the outside 76 bp of DNA per nucleosome is estimated to be  $\approx 12$  kcal/mol at 22°C based on comparison of the force–extension curves of nucleosomal and naked DNA. This value agrees rather well with a free energy value of  $\approx 10$  kcal/mol at 45–65°C, which can be derived from equilibrium restriction endonuclease accessibility data reported by Anderson and Widom (3).

In the high-force range, the disruption peaks of the force–extension curve in Fig. 1B translate into the steps seen in Fig. 2A. DNA release is sudden, with a step size of  $\approx 82$  bp. Step size was further investigated by using a force clamp that allowed for a more accurate determination (examples shown in Fig. 2B). Unlike the velocity clamp measurements, all of the nucleosomes experienced the same force before disruption. Here, sudden disruptions of nucleosomes resulted in a stepwise increase in the DNA extension, with each step corresponding to one nucleosome disruption. The steps are flat, indicating no DNA release between disruptions. The step size was uniform:  $26.3 \pm 0.5$  nm (mean  $\pm$  SEM,  $n = 28$ ) at 17.6 pN, corresponding to a DNA release of  $80 \pm 1$  bp; and  $25.5 \pm 0.4$  nm ( $n = 19$ ) at 20.2 pN, corresponding to a DNA release of  $78 \pm 1$  bp. We note that by contrast with the gradual peeling seen in the low-force range, high-force events occur as abrupt all-or-nothing events precipitated by the breaking of symmetrical bonds  $\pm 40$  bp from the dyad. Release of positive bending energy stored in the curved DNA structure constrained on the surface of the histone octamer undoubtedly makes an important contribution to the mechanism for this all-or-nothing release of DNA (21).

Our findings correlate with the relative strengths of DNA–histone interactions on the superhelical ramp of the octamer based on crystallographic data summarized by Luger and Richmond (Ref. 19; Fig. 2C). Their data show that DNA–histone interactions are symmetric about the dyad axis of the NCP. Specific DNA–histone contacts are made each time the DNA phosphodiester backbone faces the octamer surface. These contacts are strongest in the 11 bp region surrounding the dyad axis, from +5 to  $-5$  bp, and in symmetrical 11 bp regions between  $\pm 36$  and  $\pm 46$  bp positions from the dyad axis ( $\pm 1/2$  superhelical turn). Interaction strengths are much lower at DNA–histone contacts outside of these three 11 bp regions. Based on these generalizations, as nucleosomal DNA is peeled symmetrically from the surface of the octamer, a release of the outside 54 bp (26 bp from each end) is expected to occur at lower force, after which increasing resistance to peeling would be met because of the strong interactions from the  $\pm 36$  to  $\pm 46$  bp positions. Complete rupture of these strong interactions at

**Fig. 2.** The amount of DNA released from nucleosomes upon disruption. (A) Amount of naked DNA as a function of time derived from data shown in Fig. 1B. The top red dotted line is a comparison with a full-length naked DNA. At higher force, the curves show 17 steps, which correspond to the 17 disruption peaks in Fig. 1B. (B) Step size measurement using a force clamp. The graphs are plots of DNA extension vs. time under constant force. Two examples of the measurements are shown corresponding to two different forces. (C) Map of the critical DNA–histone interactions within an NCP. (Upper) Spatial map of the strongest DNA–histone interaction regions along DNA associated with the histone octamer (16). (Lower) Cartoon representation of a partially disrupted core particle.

higher force should result in abrupt release of the inner superhelical turn of DNA up to the  $\pm 5$  bp region around the dyad axis. Consistent with these predictions from structure data, we observed an initial release of  $\approx 76$  bp of DNA at low but increasing force, and abrupt release of  $\approx 80$  bp of DNA at high force, presumably corresponding to the disruption of strong DNA-histone interactions at positions  $\pm 40$  bp from the dyad axis.

**Observation of Reversible Assembly.** After disruption of bonds in the  $\pm 36$  to  $\pm 46$  bp regions, DNA should continue to be released up to the  $\pm 5$  bp positions. However, the structure of the NCP (19) shows that histones do not bend DNA significantly between the  $\pm 5$  bp positions, which will permit the strong protein-DNA contacts about the dyad to be maintained in our experiments even after DNA from the core particle is fully extended. Thus, if sufficient force were applied to DNA to mechanically peel it from the octamer surface only up to the  $\pm 5$  bp positions, the core particle might reassemble upon relaxation of the DNA. By contrast, if helix-distorting force were applied, complete dissociation of octamer and DNA might result in core particle disruption without reassembly after relaxation. Our measurements, which are sensitive to protein alterations of effective DNA length, would indicate the same amount of DNA released for both of the two possibilities described: disruption up to the  $\pm 5$  bp positions and complete dissociation of the histones from the DNA. However, repeated stretching of the same array should distinguish completely dissociated core particles from those minimally bound at the  $\pm 5$  bp positions.

Fig. 3 shows results of repeated stretching experiments carried out under conditions similar to those in Fig. 1B, except that a nucleosomal array was repetitively stretched with a 10-s relaxation period after the end of each stretch. At the end of each stretch, the DNA always had the same extension as that of the full-length naked DNA. When the final force at the end of a stretch was limited to less than 50 pN, as predicted, core particles reversibly assembled upon relaxation and new sawtooth patterns appeared in subsequent stretches. The number of disruption peaks decreased with each subsequent stretch, indicating a partial loss of histone octamers with each stretch. Once all nucleosomes had been displaced from the DNA (Fig. 3B, blue curve), the force-extension curve was the same as that of a full-length naked DNA molecule.

Our overall results contrast significantly with those from Benninck *et al.* (7). In our studies, force-extension relations clearly have the resolution to follow distinct phases of nucleosome disruption and show a periodic sawtooth pattern of  $\approx 27$ -nm spacing in the high-force range, corresponding to a uniform DNA release of  $\approx 80$  bp at each disruption. In contrast, the Benninck *et al.* data seems to show quantized steps (disruptions of single or multiple  $\approx 65$ -nm steps), but the data are not of sufficient resolution to observe each step or provide information about the various stages of disruption that we report here. Also, we observed reversible nucleosome assembly upon relaxation that was not observed in their studies. Possibly, these results differ because of the lower resolution of their instrument combined with complications caused by the presence of various DNA-binding proteins in their samples.

**Determination of Nucleosome Disruption Kinetics at  $\pm 40$  bp.** The strength and spatial extent of the strong interactions at the  $\pm 40$  bp positions were investigated further by using dynamic force spectroscopy (DFS; for review, see ref. 22). The basic idea behind DFS is straightforward: a bond will rupture if given sufficient time. However, rupture may be greatly facilitated by the application of an external force ( $F$ ), which tilts the energy landscape and thus lowers the activation barrier for bond disruption (Fig. 4A). If the applied force is increased at a constant rate (i.e., the loading rate  $dF/dt = \text{constant}$ ), and under

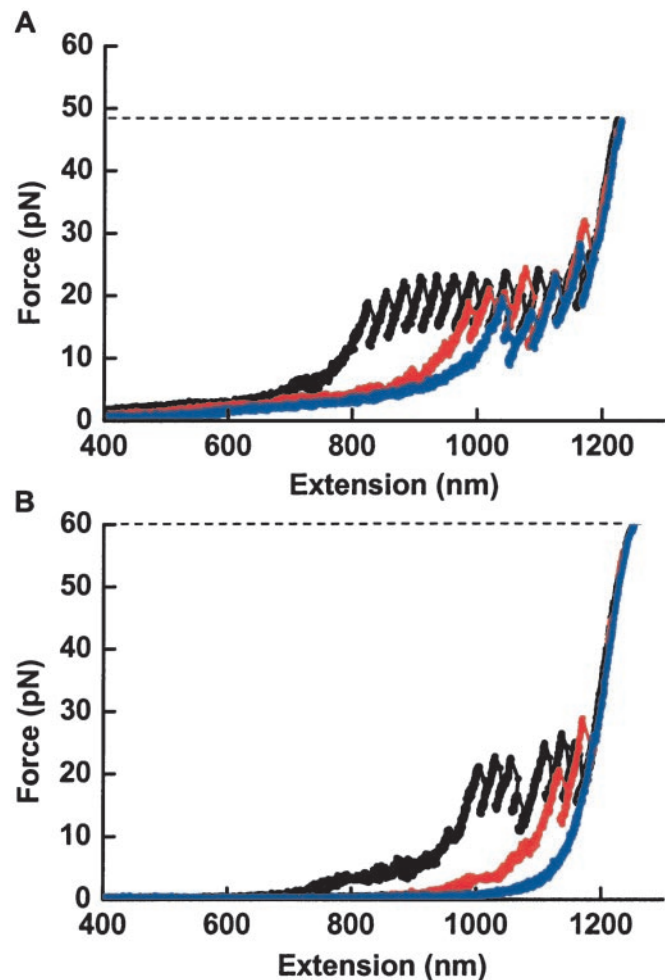


**Fig. 3.** Nucleosome reassembly after disruption by repetitive stretching with a velocity clamp. Nucleosomes were repetitively stretched with a 10-s relaxation period after each stretch. (A) Maximum force at  $\approx 50$  pN. Force-extension curves of a nucleosomal array repetitively stretched three times with maximum force at  $\approx 50$  pN: first stretch (black), second stretch (red), and third stretch (blue). (B) Maximum force at  $\approx 60$  pN. A nucleosomal array first was stretched to a maximum force of 50 pN (black). In subsequent stretches (red then blue), the maximum force was increased to  $\approx 60$  pN.

the assumption that the disruption of different nucleosomes is not cooperative, the most probable force for disruption,  $F^*$ , increases with the logarithm of  $1/N dF/dt$ , the loading rate normalized by  $N$ , the number of nucleosomes on the array during loading. We have performed DFS experiments in which the most probable force for nucleosomal-bond rupture at the  $\pm 40$  bp positions was measured at a series of loading rates. In these studies, force loading was controlled by using a velocity clamp (for examples, see Fig. 1B and C, and Fig. 3). For a given  $1/N dF/dt$ , rupture forces were pooled to obtain the most probable force  $F^*$  from the force distribution. The relationship between most probable force  $F^*$  and the normalized loading rate  $1/N dF/dt$  can be expressed as

$$F^* = \frac{k_B T}{d} \left[ \ln \left( \frac{1}{N} \frac{dF}{dt} \right) - \ln \left( \frac{k_B T k_D(0)}{d} \right) \right]$$

where  $k_D(0)$  is the rate constant for bond disruption under no external force,  $d$  is the distance (in nm) between the bound state and the activation-barrier peak along the direction of the applied

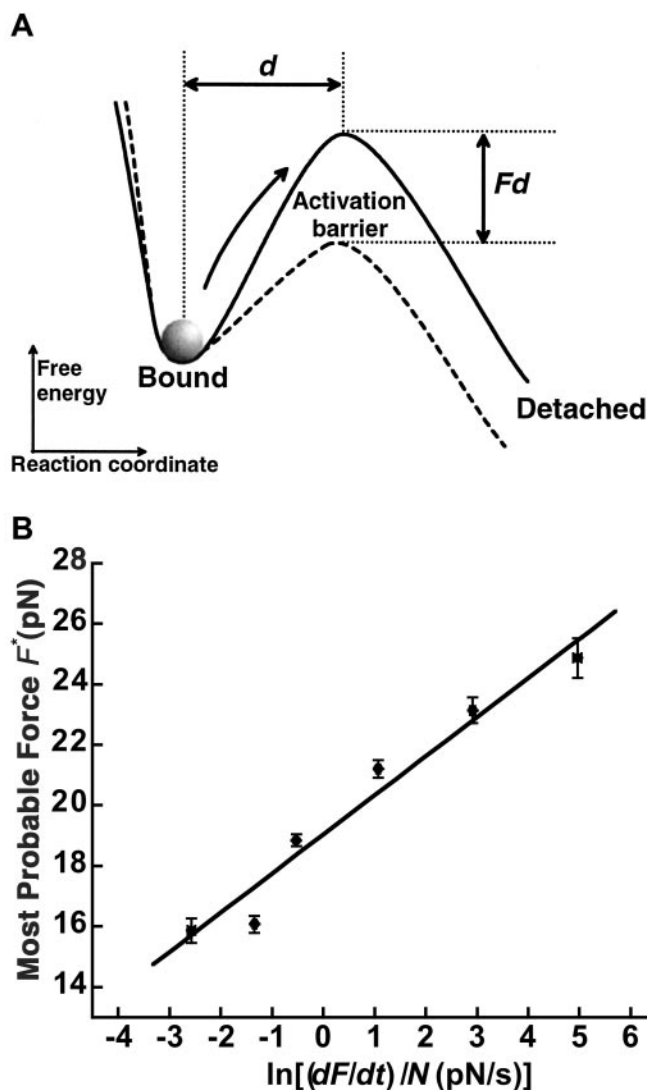


**Fig. 4.** Investigation of the strong interactions at  $\pm 40$  bp by DFS. (A) Energy diagram illustrating the basic principle of DFS. The effect of an external stretching force exerted along the reaction coordinate is to lower the height of the activation barrier between the bound and detached states. (B) A plot of most probable force  $F^*$  vs.  $\ln[1/N dF/dt]$  and its linear fit.

load (see Fig. 4A),  $k_B$  is Boltzman's constant, and  $T$  is the absolute temperature.

As can be seen from the above expression, two important parameters, the zero-load disruption rate constant  $k_D(0)$  and the bond rupture distance  $d$ , can be obtained by measuring the relation between  $F^*$  and  $1/N dF/dt$ . Fig. 4B shows a plot of  $F^*$  vs.  $\ln[1/N dF/dt]$  for all of the loading rates explored in our experiments. The best fit to the above expression yields  $d = 3.2$  nm and  $k_D(0) = 3 \times 10^{-7} s^{-1}$  under our experimental conditions. The value of  $d$  gives a measure of the distance that must be moved to disrupt strong interactions at  $\pm 40$  bp;  $d = 3.2$  nm is reasonable given the dimensions of the NCP (2).  $k_D(0)$  is small, as would be expected for the stable DNA-protein structure of the nucleosomal core particle.  $k_D(0)$  also can be converted to the height of the activation barrier  $E_b$  (see Fig. 4A) by using the expression  $k_D(0) = k_0 e^{-E_b/k_B T}$ . Because the prefactor  $k_0$  is typically  $10^9$ - $10^{10} s^{-1}$  under overdamped conditions (20),  $E_b$  for the  $\pm 40$ -bp interactions is estimated to be  $36$ - $38 k_B T$  or  $21$ - $22$  kcal/mol. This large activation barrier provides resistance to

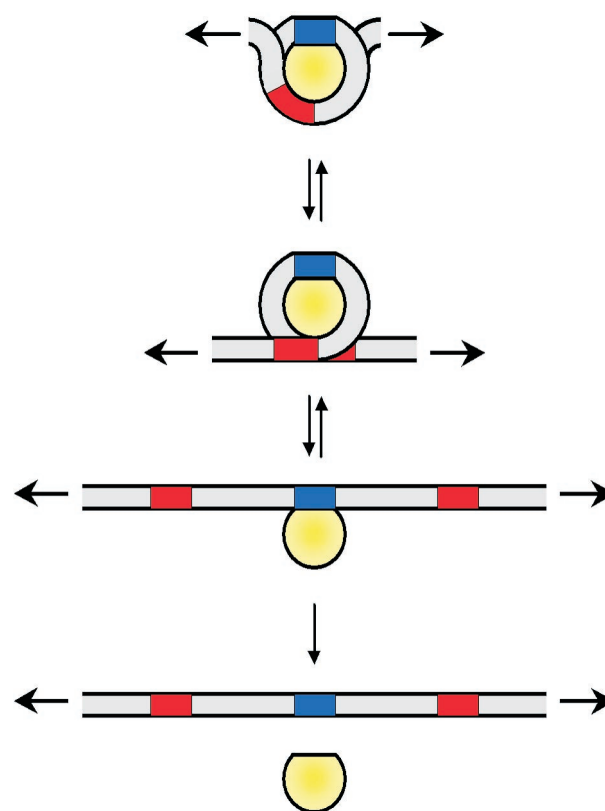


**Fig. 5.** A three-stage model for the mechanical disruption of the NCP. See text for a description.

DNA release and contributes significantly to the stability of a nucleosome.

**Stepwise Model of Forced Nucleosome Disruption.** Based on our findings, we propose a three-stage disruption model in which exit and entry DNA is peeled symmetrically from the histone octamer (Fig. 5). The first stage of disruption releases 76 bp of the external DNA (see Fig. 5). The disruption is gradual, and only low force is required to peel DNA from the protein surface. The second and third stages of the disruption involve the sudden release of the next 80 bp of DNA. The second stage of disruption is sudden because of the strong interactions presumed to be around the  $\pm 40$  bp positions. Disruption up to this point is reversible—upon DNA relaxation, the peeled DNA may reassemble onto the octamer. The third stage of disruption occurs at an even higher load, releases the remaining 11 bp of DNA, and results in a complete dissociation of the histones from the DNA. This stage is irreversible under infinite dilution of free histones in solution.

The three-stage model of nucleosome opening presented here suggests a way in which nucleosomes perform their dual functions in the eukaryotic cell, both to maintain DNA in a condensed state and to provide regulated access to the information contained therein. Although the histone octamer interacts stably with the DNA it organizes, this interaction is composed of a complex group of bond strengths arranged so as to provide progressive access to nucleosomal DNA. Enzymatic mechanisms operating on DNA can invade a nucleosome from the ends with minimal force. Stable interaction of the histone octamer and DNA is maintained in the face of this initial invasion by strong interactions that protect the inner superhelical turn. Use of greater force permits invasion of one half of the inner turn. At the centerpoint of the nucleosomal DNA, greater force (or

perhaps topological distortion) permits access to the second half of the inner superhelical turn and histone reassociation with donor DNA in the vacated half.

What is then required for access to nucleosomal DNA is a set of enzymatic mechanisms that can generate force, modify histone chemistry, and/or alter DNA topology. *E. coli* RNA polymerase has been shown to be a processive molecular motor capable of generating forces and displacements (12, 13). The RNA polymerase II motor also is expected to be capable of generating forces that overcome obstacles during translocation and is thus a source of peeling force for nucleosomal invasion. The destabilization of chromatin structure and subsequent increase in polymerase access achieved by covalent modifications such as acetylation has been documented (23, 24). Chromatin-remodeling machines like SWI/SNF, whose motor subunits are members of the helicase family of proteins, are known to modify the structure of nucleosomes by perturbing DNA-protein interactions and by inducing topological changes in nucleosomal

DNA that are conducive to transcriptional activation (25, 26). Likewise, other members of the helicase family which, unlike chromatin-remodeling machines, possess a strand-separating activity, also have been found to destabilize nucleosome structure (27, 28). Single-molecule mechanical techniques should be powerful tools for the study of chromatin and these molecular modifiers of its structure.

We thank Steven J. Koch and Alla Shundrovsky for their participation in the construction of the optical trapping setup used in these studies, and Dr. Robert M. Fulbright for his help with the data acquisition and analysis. We also thank Dr. W. Lee Kraus and Dr. Karen Adelman for advice essential to the completion of this project. This work was supported by grants from the National Institutes of Health (to J.T.L., C.L.P., and M.D.W.), the Damon Runyon Scholar Award (to M.D.W.), the Beckman Young Investigator Award (to M.D.W.), the Alfred P. Sloan Research Fellow Award (to M.D.W.), and the Keck Foundation's Distinguished Young Scholar Award (to M.D.W.). R.C.Y. was supported also by a National Institutes of Health Biophysics Training Grant to Cornell University.

1. Kornberg, R. & Thomas, J. (1974) *Science* **184**, 865–868.
2. Luger, K., Mader, A., Richmond, R., Sargent, D. & Richmond, T. (1997) *Nature (London)* **389**, 251–260.
3. Anderson, J. & Widom, J. (2000) *J. Mol. Biol.* **296**, 979–987.
4. Furrer, P., Bednar, J., Dubochet, J., Hamiche, A. & Prunell, A. (1995) *J. Struct. Biol.* **114**, 177–183.
5. Cui, Y. & Bustamante, C. (2000) *Proc. Natl. Acad. Sci. USA* **97**, 127–132.
6. Ladoux, B., Quiivy, J., Doyle, P., du Roure, O., Almouzni, G. & Viovy, J. (2000) *Proc. Natl. Acad. Sci. USA* **97**, 14251–14256. (First Published December 12, 2000; 10.1073/pnas.250471597)
7. Bennink, M., Leuba, S., Leno, G., Zlatanova, J., de Grooth, B. & Greve, J. (2001) *Nat. Struct. Biol.* **8**, 606–610.
8. Nightingale, K., Dimitrov, S., Reeves, R. & Wolffe, A. (1996) *EMBO J.* **15**, 548–561.
9. Dong, F., Hansen, J. & van Holde, K. (1990) *Proc. Natl. Acad. Sci. USA* **87**, 5724–5728.
10. Logie, C. & Peterson, C. (1997) *EMBO J.* **16**, 6772–6782.
11. Schwarz, P. & Hansen, J. (1994) *J. Biol. Chem.* **269**, 16284–16289.
12. Walter, P., Owen-Hughes, T., Cote, J. & Workman, J. (1995) *Mol. Cell. Biol.* **15**, 6178–6187.
13. Wang, M., Schnitzer, M., Yin, H., Landick, R., Gelles, J. & Block, S. (1998) *Science* **282**, 902–907.
14. Yin, H., Wang, M., Svoboda, K., Landick, R., Gelles, J. & Block, S. (1995) *Science* **270**, 1635–1637.
15. Visscher, K., Schnitzer, M. & Block, S. (1999) *Nature (London)* **400**, 184–189.
16. Rief, M., Gautel, M., Oesterhelt, F., Fernandez, J. & Gaub, H. (1997) *Science* **276**, 1109–1112.
17. Oberhauser, A., Hansma, P., Carrion-Vazquez, M. & Fernandez, J. (2001) *Proc. Natl. Acad. Sci. USA* **98**, 468–472. (First Published January 9, 2001; 10.1073/pnas.021321798)
18. Wang, M., Yin, H., Landick, R., Gelles, J. & Block, S. (1997) *Biophys. J.* **72**, 1335–1346.
19. Luger, K. & Richmond, T. (1998) *Curr. Opin. Struct. Biol.* **8**, 33–40.
20. van Holde, K. & Zlatanova, J. (1999) *BioEssays* **21**, 776–780.
21. Marky, N. & Manning, G. (1995) *J. Mol. Biol.* **254**, 50–61.
22. Evans, E. (2001) *Annu. Rev. Biophys. Biomol. Struct.* **30**, 105–128.
23. Anderson, J., Lowary, P. & Widom, J. (2001) *J. Mol. Biol.* **307**, 977–985.
24. Tse, C., Sera, T., Wolffe, A. & Hansen, J. (1998) *Mol. Cell. Biol.* **18**, 4629–4638.
25. Gavin, I., Horn, P. & Peterson, C. (2001) *Mol. Cell* **7**, 97–104.
26. Havas, K., Flaus, A., Phelan, M., Kingston, R., Wade, P., Lilley, D. & Owen-Hughes, T. (2000) *Cell* **103**, 1133–1142.
27. Ramsperger, U. & Stahl, H. (1995) *EMBO J.* **14**, 3215–3225.
28. Eggleston, A., O'Neill, T., Bradbury, E. & Kowalczykowi, S. (1995) *J. Biol. Chem.* **270**, 2024–2031.